Complex phase ordering of the one-dimensional Heisenberg model with conserved order parameter

R. Burioni
Dipartimento di Fisica and INFN, Università di Parma, Parco Area delle Scienze 7/A, I-423100 Parma, Italy

F. Corberi
Dipartimento di Matematica ed Informatica via Ponte don Melillo, Università di Salerno, 84084 Fisciano (SA), Italy

A. Vezzani
Dipartimento di Fisica, S3, National Research Center, CNR-INFM, via Campi 213/a, 41100 Modena, Italy and Dipartimento di Fisica, Università di Parma, Parco Area delle Scienze 7/A, I-423100 Parma, Italy

(Received 21 May 2008; revised manuscript received 5 February 2009; published 13 April 2009)

We study the phase-ordering kinetics of the one-dimensional Heisenberg model with conserved order parameter by means of scaling arguments and numerical simulations. We find a rich dynamical pattern with a regime characterized by two distinct growing lengths. Spins are found to be coplanar over regions of a typical size $L_V(t)$, while inside these regions smooth rotations associated to a smaller length $L_C(t)$ are observed. Two different and coexisting ordering mechanisms are associated to these lengths, leading to different growth laws $L_V(t) \sim t^{1/3}$ and $L_C(t) \sim t^{1/4}$ violating dynamical scaling.

DOI: 10.1103/PhysRevE.79.041119 PACS number(s): 05.70.Ln, 75.40.Gb, 05.40.−a

I. INTRODUCTION

After quenching a ferromagnetic system to a low-temperature phase, relaxation toward the new equilibrium state is realized by a progressive phase-ordering [1]. The specific mechanisms involved in the coarsening phenomenon depend on the presence and the nature of topological defects. In d-dimensional systems described by an $\mathcal{O}(N)$ vector order parameter, topological defects are unstable for $N > d+1$ (for $N=d+1$ peculiar defects as textures [2] may be present). Therefore, in the asymptotic regime when all defects have disappeared, the dynamics is solely driven by the reduction in the excess energy related to the smooth rotations of the order parameter. In contrast, systems with $N \leq d$ are characterized by the presence of stable defects whose presence influences the dynamics in the whole phase-ordering stage. In particular, when $N=d$ defects are localized and ordering occurs by mutual defect-antidefect annihilation. This is the case of the Ising chain, where up and down domains are separated by pointlike interfaces performing random walks.

Generally, the late stage is characterized by dynamical scaling [1,3]. This implies that a single characteristic length $L(t)$ can be associated to the development of order in such a way that configurations of the system are statistically independent of time when lengths are measured in units of $L(t)$. The characteristic length usually has a power-law growth $L(t) \propto t^{1/z}$. In systems with a conserved order parameter (COP) one generally finds $z=3$ [4,5] or $z=4$ [6,5] for $N=1$ and $N>1$ respectively.

For systems at or below the lower critical dimension d_L, such as the Ising chain, a true asymptotic phase ordering can only be observed in quenches to $T=0$. However, if quenches to a relatively low temperature are performed, one observes an initial transient regime (but very long lasting when T is small) where the dynamics is indistinguishable from that at $T=0$. This regime lasts until $L(t)$ has grown comparable to the equilibrium coherence length $\xi(T)$.

In this paper, we investigate the phase-ordering kinetics of the one-dimensional Heisenberg model ($N=3$) with COP quenched to a low temperature T. We show that the dynamics is much richer than what one would naively expect. This is due to the formation, in an early stage, of couples of parallel spins, separating regions in which the spins are coplanar. These parallel spins act as pointlike defects, as it will be explained in Sec. III. Their presence provides an analogy between the Heisenberg and the Ising chains, where couples of parallel spins and regions of coplanarity in the former model correspond to interfaces and domains in the latter. The analogy is not only formal but is reflected in the kinetics: in a first stage (whose duration however diverges in the $T \to 0$ limit) regions of coplanar spins coarsen similarly to the domains of the Ising model, with their typical length growing as

$$L_V(t) \sim t^{1/3}. \tag{1}$$

In this regime the number of defects is reduced only by a mechanism which recalls the annihilation of the interfaces in the Ising model. Simultaneously, smooth rotations of the spins, typical of vectorial systems, occur inside the regions of coplanarity. The coherence of the spins inside these regions extends over a length $L_C(t) \ll L_V(t)$ increasing as

$$L_C(t) \sim t^{1/4}. \tag{2}$$

The existence of two growing length, associated to different ordering mechanisms, produces the breakdown of dynamical scaling. In the analogy between the Heisenberg and the Ising chains, a notable difference must be stressed. While in the latter interfaces are stable defects which can only be removed by mutual annihilation, defects in the former are unstable. Namely, after a first stage of coarsening of coplanar regions, the defects spontaneously decay due to thermal fluctuations. The typical lifetime of the defects is limited by

temperature and coarsening of the coplanar regions persists up to very long times in deep quenches. After that, defects disappear and the system finally enters a late stage where smooth spin rotations remains the only mechanism at work, until equilibration is attained when $L_C(t) \sim \xi(T)$. In this regime dynamical scaling is restored with exponent $z=4$, as expected for a system with $N > d+1$. In the small-temperature limit the duration of the two regimes, with and without dynamical scaling, is comparable.

This paper is organized as follows. In Sec. II we introduce the model and define the observable quantities that will be considered. In Sec. III we describe the main features of the dynamics in the different regimes, compute the value of the exponents and of other quantities by means of scaling arguments, and compare our results with the outcome of numerical simulations of the model. A summary and the conclusions are contained in Sec. IV.

II. MODEL AND OBSERVABLES

The Heisenberg model is defined by the Hamiltonian

$$H[\sigma] = \sum_{i=1}^{\mathcal{N}} \epsilon_i = -J \sum_{i=1}^{\mathcal{N}} (\vec{\sigma}_i \cdot \vec{\sigma}_{i+1} - 1) = -J \sum_{i=1}^{\mathcal{N}} (\cos \phi_i - 1), \tag{3}$$

where ϵ_i is the local energy density, $\vec{\sigma}_i$ is a three-component unit vector spin, $i=1,\ldots,\mathcal{N}$ are the sites on a one-dimensional lattice, and ϕ_i is the angle between $\vec{\sigma}_i$ and $\vec{\sigma}_{i+1}$. We will assume $J=1$ and the Boltzmann constant $k_B=1$.

The equilibrium properties of the model are exactly known [7]. This system is ergodic except at $T=0$. At any finite temperature the state is disordered with a vanishing magnetization and internal energy (per spin) $E_{\rm eq}(T)=T-\coth(1/T)+1$ with the low-temperature expansion $E_{\rm eq}(T) \simeq T$. The correlation function $C_{\rm eq}(r)=\langle \vec{\sigma}_i \vec{\sigma}_{i+r} \rangle = [1-E_{\rm eq}(T)]^r$ decays exponentially over a coherence length $\xi(T)$ that diverges in the $T \to 0$ limit.

Concerning dynamics, at equilibrium the model possesses an intrinsic kinetics where the energy and the magnetization are conserved [8]. Studies [9] of this intrinsic dynamics have evidenced the failure of the equilibrium scaling symmetry close to $T=0$. Experimental work supports this picture [10].

For the situation considered here, where the system is quenched from a high-temperature configuration to a low temperature T, a different dynamics allowing transfer of energy to a heat bath must be considered. In order to model this, we introduce a dynamics where two neighboring spins $\vec{\sigma}_i, \vec{\sigma}_{i+1}$ of a configuration $[\vec{\sigma}]$ are randomly chosen at each time step and then they are updated to $\vec{\sigma}'_i, \vec{\sigma}'_{i+1}$ provided the local magnetization is conserved, namely, $\vec{s}_i = \vec{\sigma}_i + \vec{\sigma}_{i+1} = \vec{\sigma}'_i + \vec{\sigma}'_{i+1}$. Notice that magnetization is conserved at the local level with this rule. Due to the conservation law, the spins $\vec{\sigma}_i, \vec{\sigma}_{i+1}$ can only rotate rigidly around their sum $\vec{s}_i$, as shown in Fig. 1. We consider the heat-bath transition rates $[\vec{\sigma}] \to [\vec{\sigma}']$ satisfying detailed balance

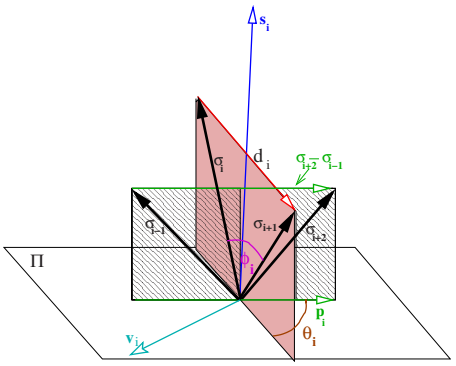

FIG. 1. (Color online) Schematic representation of the four spins $\vec{\sigma}_{i-1}, \vec{\sigma}_i, \vec{\sigma}_{i+1}, \vec{\sigma}_{i+2}$.

$$w_i[\vec{\sigma}'] = W_i^{-1} \exp\left(-\frac{H[\vec{\sigma}']}{T}\right), \tag{4}$$

where $W_i = \int d\vec{\sigma}'_i d\vec{\sigma}'_{i+1}\, \delta(\vec{\sigma}_i + \vec{\sigma}_{i+1} - \vec{s}_i) \exp(-H[\vec{\sigma}']/T)$. Heat-bath transition rates provide a particularly fast and efficient dynamics with respect to other (i.e., METROPOLIS) choices [11]. Let us denote $\vec{d}_i = \vec{\sigma}_{i+1} - \vec{\sigma}_i$, $\vec{d}'_i = \vec{\sigma}'_{i+1} - \vec{\sigma}'_i$, and $\vec{p}_i$ as the projection of $\vec{\sigma}_{i+2} - \vec{\sigma}_{i-1}$ on the plane Π perpendicular to $\vec{s}_i$ (see Fig. 1). Any move, involving the couple $\vec{\sigma}_i$ and $\vec{\sigma}_{i+1}$, can be described by a rotation in the plane Π from $\vec{d}_i$ to $\vec{d}'_i$. In this framework the angles between $\vec{p}_i$ and $\vec{d}_i$ ($\vec{d}'_i$), denoted as θ_i (θ'_i), fully parametrize the dynamics and the transition rate (4) can be rewritten as

$$w_i(\theta'_i) = W_i^{-1} \exp\left(\frac{d_i p_i (\cos\, \theta'_i - 1)}{2T}\right), \tag{5}$$

where $d_i = |\vec{d}_i| = |\vec{d}'_i|$ and $p_i = |\vec{p}_i|$. Von Neuman rejection method [12] allows us to efficiently generate θ'_i according to the transition rates (5). Notice that in a move the typical deviations from the lowest-energy configuration ($\theta'_i = 0$) are of order

$$\cos\, \theta'_i - 1 \sim \frac{2T}{d_i p_i}. \tag{6}$$

We consider a system initially prepared in a high-temperature uncorrelated state, with $\sum_{i=1}^{\mathcal{N}} \vec{\sigma}_i = 0$, and then quenched, at time $t=0$, to a lower final temperature T. As already mentioned in Sec. I, the dynamics of systems at or below the critical dimension, such as the one considered here, is characterized by an initial transient where the system orders [13,14] as in a quench to $T=0$. The characteristic length of ordered regions grows in time until, at time $\tau_{\rm eq}(T)$, it becomes comparable to $\xi(T)$. At this point the final equilibrium state at T is entered and phase ordering ends. If the system is quenched to a sufficiently low temperature, since $\xi(T)$ is very large, the phase-ordering kinetics extends over a huge time window $t < \tau_{\rm eq}(T)$.

Characteristic lengths, and scaling properties, can be studied from the knowledge of the two-point equal-time correlation function

$$C(r,t) = \langle \vec{\sigma}_i(t) \cdot \vec{\sigma}_{i+r}(t) \rangle, \tag{7}$$

where $\langle \cdots \rangle$ means an ensemble average, namely, taken over different initial conditions and thermal histories. Due to space homogeneity, $C(r,t)$ does not depend on i. Dynamical scaling [1] would imply

$$C(r,t) = c(x), \tag{8}$$

where $x = r/L(t)$. For systems with an $\mathcal{O}(N)$ vector order parameter the Bray-Puri-Toyoki [15] behavior

$$1 - c(x) \sim x^N \tag{9}$$

is observed for small x. In the scalar case, this behavior reduces to the Porod's law [16]

$$1 - c(x) \sim x, \tag{10}$$

which is generally expected in systems with sharp interfaces. From Eq. (8) one can extract a quantity $L_C(t)$ proportional to $L(t)$ from the condition

$$C[L_C(t),t] = \frac{1}{2}, \tag{11}$$

namely, as the half-height width of $C(r,t)$. In the following we will also consider the correlation

$$V(r,t) = \langle \vec{v}_i(t) \cdot \vec{v}_{i+r}(t) \rangle, \tag{12}$$

where the unit vectors

$$\vec{v}_i = \frac{\vec{\sigma}_i \times \vec{\sigma}_{i+1}}{|\vec{\sigma}_i \times \vec{\sigma}_{i+1}|} \tag{13}$$

identify the planes formed by neighboring spins; hence, $V(r.t)$ represents the correlations between these planes. When scaling holds, $V(r,t)$ behaves similarly to $C(r,t)$, namely,

$$V(r,t) = v(x) \tag{14}$$

and, defining $L_V(t)$ analogously to $L_C(t)$ in Eq. (11), also $L_V(t) \propto L(t)$.

III. DYNAMICS: SCALING ARGUMENTS AND NUMERICAL RESULTS

In the following we will discuss the main features of the dynamical process by means of scaling arguments and numerical simulations. These are performed on a string of 8000 spins with periodic boundary conditions $\sigma_{\mathcal{N}+1} = \sigma_1$. We have checked that with this size our simulations are free from finite-size effects. An average of over five to ten realizations is made for each simulation. In the limit of low temperatures, to which we are interested in, the kinetics becomes very slow since, as it will be discussed below, time rescales as $T^{-1/2}$; simulations are therefore quite time consuming in this region. The dynamics of a low-temperature quench is characterized by different subsequent regimes, which are separately discussed below.

A. Pinning (quenches to $T=0$)

The kinetics of the quench to $T=0$ is determined by the existence of frozen states where the system gets trapped after a while. The nature of these states can be understood by looking at the first line (denoted as time t) of Fig. 2. The two spins on sites $i, i+1$ are parallel; hence, no move involving this couple can be done since the angle θ_i is not defined. On the left and on the right of the aligned spins there are regions where the spins are coplanar, and hence $\vec{v}_i$ are parallel and point along certain directions, denoted by α, β, etc., which can be considered as different *phases* of the system. These phases extend up to another couple of parallel spins (not shown in the figure). As it will be shown in Sec. III C, in quenches to finite temperatures the system depins after a while and these coplanar regions coarsen much in the same way as equilibrium phases do in usual coarsening systems. Due to this analogy, the term phases are used also here. However it must be noticed that regions of coplanarity are not equilibrium phases, because in equilibrium spins are coplanar and aligned, while here they typically rotate (see Fig. 2), as will be discussed in Sec. III C. For the following discussions, we also introduce the terminology *distance* between two phases α, β related to the angle by which the vectors $\vec{v}_i$ of the phase α must rotate in order to align with those of the phase β. In this sense we will also talk of *nearby* or *distant* phase.

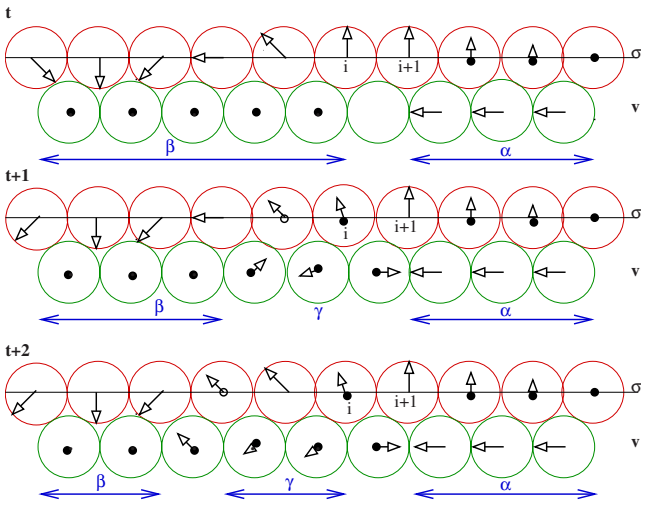

FIG. 2. (Color online) Schematic representation of spin configurations at three subsequent times $t, t+1, t+2$. For each time the upper and lower lines represent the $\vec{\sigma}$ and $\vec{v}$ configurations. Given a vector $\vec{\sigma}$ (or $\vec{v}$) with components (a,b,c), the arrow in the figure is a vector of components $(a,b,0)$, namely, the projection of $\vec{\sigma}$ on the two-dimensional plane of the figure. The third component c can be read off by the constraint of unitary length of $\vec{\sigma}$ with the help of the unitary circles represented around each vector. The origin of a vector is marked with a heavy dot when $c<0$ (vector pointing behind the figure) or with an open circle when $c>0$. The meaning of the *phases* α, β, γ is discussed in the text.

As anticipated in Sec. I, the impossibility to eliminate couples of parallel spins by means of local rearrangements, involving $\vec{\sigma}_i, \vec{\sigma}_{i+1}$ alone, makes them reminiscent of topological defects. Actually these spins represent real topological defects as is readily seen by considering the representation in terms of $\vec{v}_i$ instead of $\vec{\sigma}_i$. With this description, phases are domains in a strict sense, namely, $\vec{v}_i$ is constant in the interior of coplanar regions. They will be denoted as *domains*

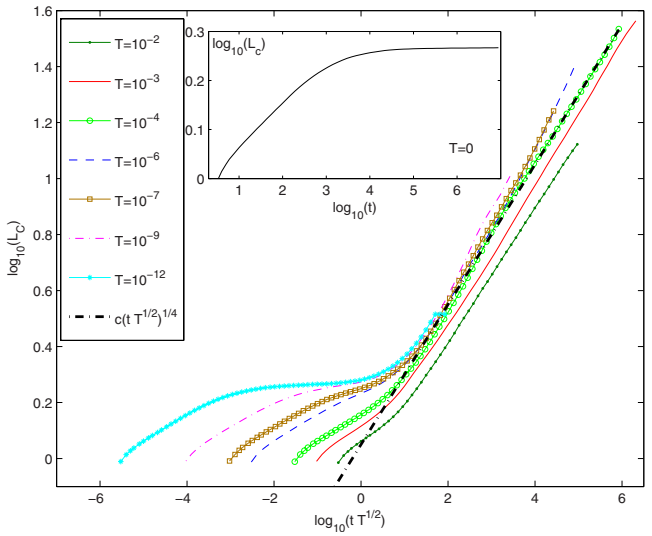

FIG. 3. (Color online) The quantity $L_C(t)$ is plotted against rescaled time $tT^{1/2}$ for different temperatures. The dotted-dashed line is the expected behavior $L_C(t) \propto (tT^{1/2})^{1/4}$ after the depinning (see text). In the inset the same quantity is plotted against time in the case $T=0$.

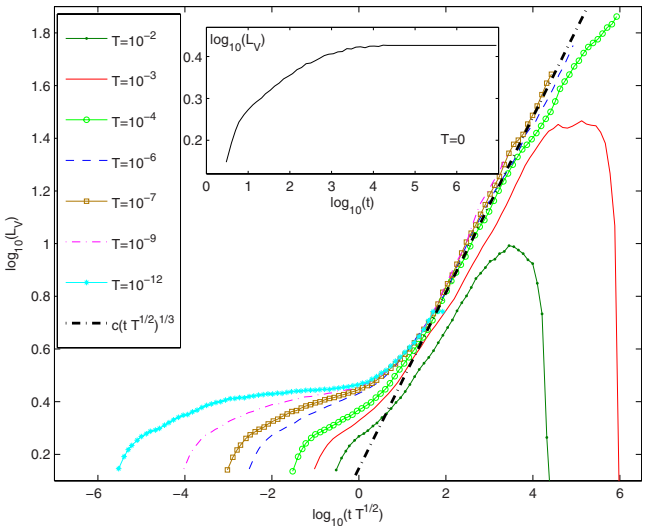

FIG. 4. (Color online) The quantity $L_V(t)$ is plotted against rescaled time $tT^{1/2}$ for different temperatures. The dotted-dashed line is the expected behavior $L_V(t) \propto (tT^{1/2})^{1/3}$ in the first phase-ordering regime (see text). In the inset the same quantity is plotted against time in the case $T=0$.

in the following, or planes, in view of the coplanarity of their spins, without further specification. Different domains are separated by sharp boundaries and, right on top of them, there is a localized defect where $\vec{v}_i$ is not defined. Then, once the proper representation is considered, parallel spins qualify as defects in the usual sense. Since spins are coplanar inside the domains and parallel on a defect, it is clear that any move involving any couple of spins is forbidden at $T=0$, and the dynamics is frozen on states like those depicted on the first line of Fig. 2. By identifying aligned spins as defects separating domains, an analogy with the COP Ising model, which freezes as well at $T=0$ [17], can be drawn. Let us mention, however, at least two main differences. First, the constraint on the motion of parallel spins in the Heisenberg model is related to the kinetic rule and not to $T=0$. Second, as will be discussed in Sec. III D, the defects in the Heisenberg model are unstable, although their lifetime diverges in the $T \to 0$ limit.

When a quench to $T=0$ is performed, the system starts reducing its energy by ordering the spins until some couples happen to be nearly parallel. Meanwhile the n spins between two defects adapt themselves on a plane. Since n is a finite number this process can be accomplished in a finite time. At this point, the model gets trapped in one of the absorbing states discussed above. Notice that, in a situation as the one discussed here, $L_V(t)$ and $L_C(t)$ describe, respectively, the length of the domains and the coherence length of the spins in the bulk of the planes. The evolution of the model toward the pinned state can be studied by following the evolution of these lengths in the insets of Figs. 3 and 4. In a quench to $T=0$ both these quantities initially grow but then saturate to a constant value when the system freezes.

B. Depinning

When $T \neq 0$ but sufficiently small, the dynamics leading the system to the frozen state proceeds practically as in the case $T=0$ described in Sec. III A, since it is entirely dominated by the moves which lower the energy which are not affected much by a small T. When the system is trapped in the absorbing state, however, activated moves can occur inside the domains if $T>0$. According to Eq. (6), since the system is still very disordered in this stage, both d_i and p_i are on average large and the typical value $\bar{\theta}$ of the angle θ_i (we will use the overbar in the following to denote the typical value of a quantity) is small. Notice, in fact, that even for the smallest temperatures considered in the simulations reported in Figs. 3 and 4 pinning is never complete: $L_C(t)$ and $L_V(t)$ keep slowly increasing because couples of spins are tiny twisted. This mechanism eventually depins the system from the absorbing state, restoring the dynamics, as shown in Figs. 3 and 4, after a characteristic time $\tau_p(T)$. From Eq. (6), assuming $\bar{\theta}$ to be small, one has $\cos \bar{\theta} - 1 \simeq \bar{\theta}^2 \simeq 2T/(\bar{d}\bar{p})$ and hence $\bar{\theta} \sim T^{1/2}$. Since $\bar{\theta}$ is tiny, a number $n(T) \simeq \pi/\bar{\theta}$ of these moves are needed in order to produce an appreciable decorrelation (of an angle of order, say, π) with respect to the pinned state and to restart the dynamics. Therefore we find

$$\tau_p(T) \sim T^{-1/2}. \tag{15}$$

According to this result, for sufficiently low temperatures the curves for $L_C(t)$ or $L_V(t)$ (and, more generally, of any time-dependent observable) should collapse after the pinning stage when plotted against $tT^{1/2}$. Figures 3 and 4 show that this is indeed quite well verified over 10 decades in temperature (with some deviations that will be discussed in Sec. III C).

C. First phase-ordering regime: Presence of domains

Here we give a schematic description of the microscopic kinetics in a first dynamical regime occurring after the de-

pinning. In this regime spins evolve in such a way that the coplanarity of the spins inside the phases is preserved. Actually, the domains compete among themselves and grow much in the same way as the equilibrium phases in usual coarsening systems, as testified bye the increase in $L_V(t)$ (see Fig. 4). This regime lasts until the phenomenon of the breakdown of the plains, discussed in Sec. III D, occurs. [When this happens $L_V(t)$ stops growing and goes abruptly to zero. The end of this first dynamical stage can then be easily recognized by inspection of Fig. 4.]

As we will explain below, in this regime two mechanisms are at work: the former is responsible for the coarsening of the domains, while the latter is the phase ordering of the spins inside the domains. Since these mechanisms are associated to two different growing lengths, dynamical scaling is not obeyed, as we will show explicitly.

1. Coarsening of the domains

In the limit of small T, among the moves discussed in Sec. III B, those which produce the smallest energy increase are overwhelmingly favored. These are generally the moves involving the spins near the boundary of a plane, for instance, those on sites $i-1$ and i in Fig. 2. The effect of this move occurring in the β phase is the nucleation of a third phase, denoted by γ, as it is clear considering the direction of the vector $\vec{v}_{i-1}$ in the second line (denoted as time $t+1$) of the figure (a spurious phase on site $i-2$ is also generated, whose presence is, however, irrelevant). At this point the dynamics may proceed by rotating the spins $\vec{\sigma}_{i-2}, \vec{\sigma}_{i-1}$ in order to make $\vec{\sigma}_{i-2}$, $\vec{\sigma}_{i-1}$, and $\vec{\sigma}_i$ coplanar (third line, denoted as time $t+2$, in the figure). In this way the new phase γ may spread replacing the pre-existing phase β. After the complete replacement of the phase β with γ (when this occurs), if the energy of the system is increased (because γ is more distant to the neighboring phase α (or the one on the left, not shown in the figure) than the original β phase, the γ phase is quickly readsorbed by reversing the process. Conversely, if the energy of the system is decreased a new blocked state is reached, characterized by domains of more nearby phases. This mechanism provides a *direction* to the process, favoring on the average the formation of new phases for which a diminishing of the system energy occurs. At this point the process can start again with the activated nucleation of a new phase replacing γ and so on repeatedly until one of the two adjacent phases (say α) extends over the original domain of the β phase, increasing the typical size of the domains.

The basic steps of this ordering process may recall what happens in the COP Ising model [17]. Actually, in both cases there are domains of different phases ($\sigma_i = \pm 1$ in Ising and $\vec{v}_i = \alpha$, β, etc. in the Heisenberg models) separated by sharp interfaces (see also the discussion on Porod's tails below in this section). In both cases, the first step is the nucleation of a germ of another phase (the evaporation of a monomer in Ising) inside a domain of a preexistent phase. After nucleation, the kinetics proceeds by a random motion of the nucleated phase. This analogy is not only qualitative since, as we show below, the growth exponent of $L_V(t)$ is the same ($z=3$).

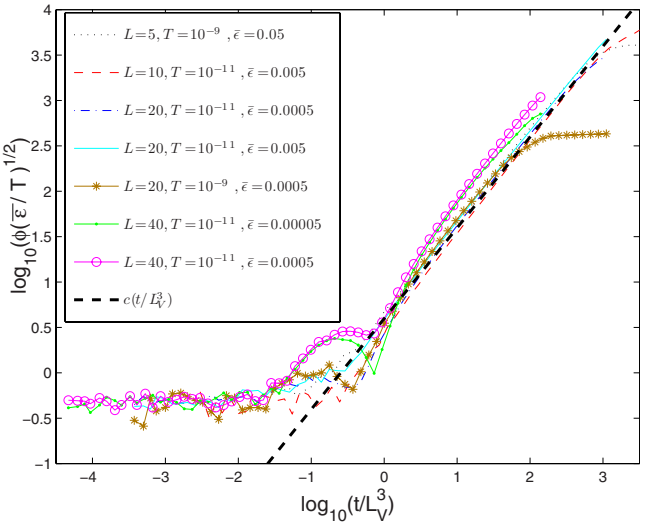

FIG. 5. (Color online) Simulation of a single domain of L_V spins. The angle ϕ of the central spin (rescaled by $T^{1/2}$) is plotted against rescaled time t/L_V^3.

Actually this can be inferred by the following argument. After the first move, the position of the boundary between the new nucleated phase γ and the remaining of the old β phase performs a random walk. Considering the long-time regime, where $L_V(t)$ is large, most of the times the boundary returns to its original position j. In this case the γ phase is readsorbed after the duration $\delta \sim L_V^2(t)$ of the random walk. The probability that the interface moves a distance $L_V(t)$ and hence the β phase is eliminated is proportional to $1/L_V(t)$ [17]; for this reason the whole process must be repeated $L_V(t)$ times in order to substitute the old phase β. This requires a time

$$\tau_\dagger \propto L_V(t)\delta \propto L_V(t)^3. \tag{16}$$

This conjecture has been tested by means of numerical simulations, mimicking the evolution of a single domain as follows. We have prepared a domain of L_V initially coplanar spins, with a uniform rotation such that $\epsilon_i = \bar{\epsilon}, \forall i$ in the bulk of the domain. The boundary condition is made of two spins (on each side) lying on a differently oriented plane. Then we started the dynamics and recorded the behavior of the central spin as a function of time for different choices of L_V and of $\bar{\epsilon}$. The results are presented in Fig. 5. The central spin can be described by a couple of angles ϕ, ψ. Here we plot the behavior of ϕ (similar results are obtained for ψ) as time passes. In an early stage $t < \tau_\dagger$ the central spin remains blocked since the dynamics starts from the boundary and proceeds toward the interior, as discussed above. Then ϕ is constant. Later, from $t = \tau_\dagger$ onward the central spin begins to rotate unless the entire plane is aligned with the plane described by the boundary conditions. This is testified by the linear increase in ϕ toward a limiting final value. The figure shows that the curves for different L_V collapse when time is rescaled as t/L_V^3. This supports Eq. (16). Notice also that, by considering different temperatures and $\bar{\epsilon}$, one obtains data collapse by plotting $\phi(\bar{\epsilon}/T)^{1/2}$. This is a consequence of Eq.

(6). Actually d_i can be written as $d_i=\sqrt{(2\epsilon_i)}$. Then $\bar{d}$ is of order $\sqrt{\bar{\epsilon}(t)}$. Analogously, it can be shown that also $\bar{p} \sim \sqrt{\bar{\epsilon}(t)}$. Inserting these typical quantities in Eq. (6), and letting $\cos\bar{\theta} \simeq 1-\bar{\theta}^2$, since in the late stage spins are rather aligned, one obtains

$$\bar{\theta} \sim \left(\frac{T}{\bar{\epsilon}}\right)^{1/2}. \tag{17}$$

In conclusion, the numerical simulation of the evolution of the single domain confirms our scaling hypothesis.

At low temperatures, as discussed above, $\bar{\theta}$ is small and hence the new generated γ phase is only slightly different from the pre-existing β. Reasoning along the same lines as regarding the simulation of a single domain, the process of replacement of an old phase with a new one must be repeated a number $n_r(T) \propto T^{-1/2}$ of times in order to obtain, in place of the original β phase, the phase (say α) of one of the neighboring domains. In conclusion, the complete replacement of the phase β with a neighboring one (α) requires a time of order $\Delta t \propto n_r(T) L_V^3$. When this process is completed the typical length of a domain is increased of a quantity $\Delta L_V(t) \propto L_V(t)$. Therefore $dL_V(t)/dt \simeq \Delta L_V(t)/\Delta t \propto L_V(t)^{-2} T^{1/2}$ and hence

$$L_V(t) \sim (tT^{1/2})^{1/3} \tag{18}$$

This prediction can be checked in Fig. 4. Here one observes that the curves for $L_V(t)$ relative to different temperature quenches collapse (after the pinning) when plotted against $tT^{1/2}$. The collapse is good for the lower temperatures (for $T \leq 10^{-4}$), while it is quite rough at higher temperatures. This is expected since our results are valid in the $T \to 0$ limit. Regarding the power growth law (18), it is satisfactorily confirmed by the data in a certain time window after the depinning. For longer times $L_V(t)$ goes abruptly to zero due to the phenomenon of the breakdown of the planes that will be discussed in Sec. III D. As explained in Sec. III D this phenomenon is delayed lowering T [actually, for a relatively high temperature as $T \geq 10^{-3}$ it prevents the observation of law (18)].

We consider now the issue of dynamical scaling. In Fig. 6 we plot $V(r,t)$ against $x=r/L_V(t)$ in the range of times in which this first dynamical regime occurs. One observes a good data collapse up to $r/L_V(t) \simeq 1.5$. According to Eq. (14), this implies that $V(r,t)$ takes a scaling form in this range of $r/L_V(t)$. Since usually scaling is first achieved for smaller distances, one could infer that, by pushing the simulations to much longer times, one could observe collapse on a larger range of $/L_V(t)$ and conclude that the whole $V(r,t)$ scales. This is surprising, since we have anticipated that dynamical scaling is violated in this regime. However this happens because the correlator $V(r,t)$, due to its construction, exclusively probes the dynamics of the boundaries of the domains, being blind with respect to the spin configuration inside, whose evolution is responsible for the breakdown of dynamical scaling, as we will discuss in Sec. III C 2. One could say that, restricting the attention on the plane boundaries, *scaling is obeyed*, although globally it is not. A similar situation is observed in the $d=1$ XY model [2] where again

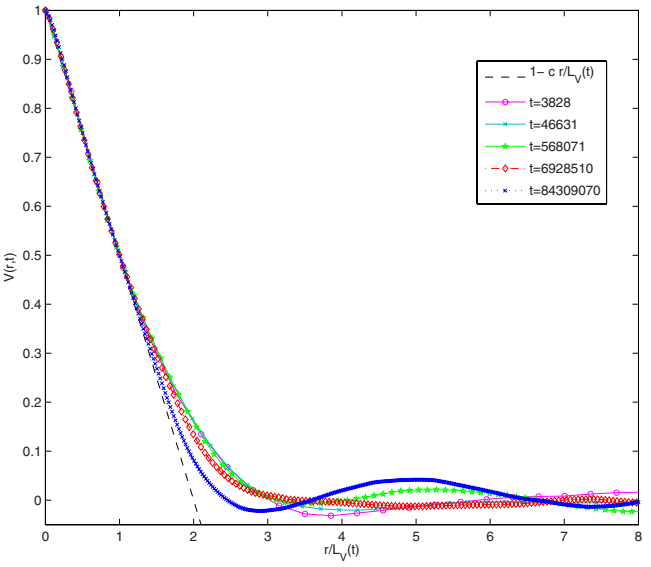

FIG. 6. (Color online) $V(r,t)$ is plotted against $r/L_V(t)$ for a quench to $T=10^{-7}$ and different times. The dashed line is the Porod law (10).

scaling does not hold (for a different reason) but particular correlators, such as $C(r,t)$ or $V(r,t)$, take scaling forms. Clearly this is not a general property of every observable, as genuine scaling should imply. Finally, the Porod law (10) is obeyed, signaling that interfaces are sharp and that domains remain well defined while coarsening in this whole regime.

2. Phase ordering of the spins

Inside the planes, the spins smoothly rotate generating textures, much like in the one dimensional XY model [2]. Comparing Figs. 3 and 4 one understands that the length $L_C(t)$ associated to the spin-spin coherence is much smaller than $L_V(t)$, particularly for large times. Then, what really matters for $L_C(t)$ is the evolution of the spins in the bulk of the domains, where, since the interfaces are far away, all the additional complications related to their presence become irrelevant. As far as the spin-spin correlations are considered, therefore, one expects the system to behave as a *normal* conserved vectorial system (but with $N=2$), namely, $C(r,t)$ to obey the scaling form (8) and Eq. (2) to hold. These features can be checked in Figs. 3 and 7. Regarding the growth law of $L_C(t)$ we obtain a behavior in good agreement with what expected, namely, Eq. (2), for the higher temperatures, namely, for $T \geq 10^{-4}$. For the lower temperatures, namely, $T \leq 10^{-7}$, we measure an effective exponent somewhat larger than 1/4. The case with $T=10^{-6}$ is somehow in between since the curve initially (after the pinning) grows with an exponent larger than 1/4 but then the slope is gradually reduced and an exponent in agreement with 1/4 is obtained toward the end of the simulation. The behavior of this curve may probably provide an interpretation for what is observed for the lower temperatures. Namely, the behavior seems to set in after a transient which widens as T is lowered. In the transient a slightly larger exponent is observed. Notice that the curves for $L_C(t)$ roughly collapse (we recall that the figure covers 10 decades in T) when plotted against $tT^{1/2}$, for the same reason of $L_V(t)$.

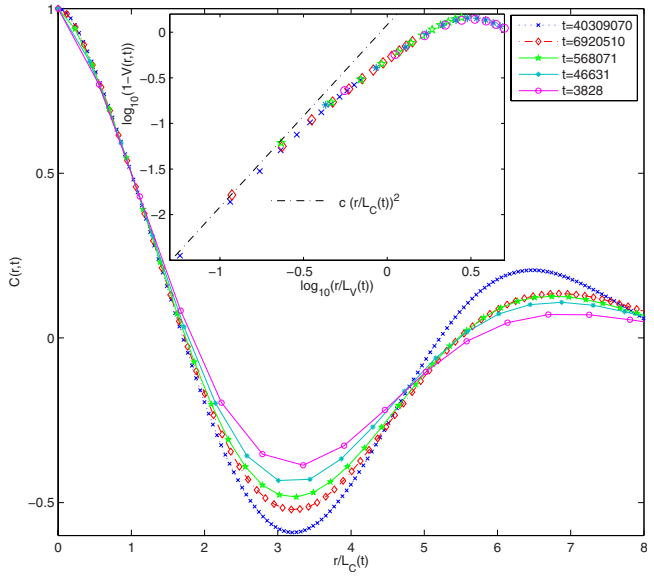

FIG. 7. (Color online) $C(r,t)$ is plotted against $r/L_C(t)$ for a quench to $T=10^{-7}$ and different times. The dashed line is the Porod law (10). In the inset, $1-C(r,t)$ is plotted against $r/L_C(t)$ on a double logarithmic scale. The dotted-dashed line is the form (9) with $N=2$.

Similarly, the collapse seems to improve in quality as $T \to 0$, as expected, while for $T \geq 10^{-3}$ the collapse is poor.

The scaling form (8) can be checked in Fig. 7. Here one observes a good data collapse up to $r/L_C(t) \simeq 1.5$, similarly to what is observed for $V(r,t)$. Concerning the shape of $C(r,t)$, differently from $V(r,t)$ it does not display the Porod's tail, as expected since the rotation of the spins is smooth and there are no sharp interfaces. On the other hand, one observes (in the inset) behavior (9) typical of vectorial systems but, interestingly, with an *effective* value $N=2$ which is clearly interpreted as due to the fact that spins in this regime lie on planes.

The results discussed insofar provide a picture of a system with two different ordering mechanisms at work, coarsening of the planes and phase ordering of the spins. These profoundly different processes coexist in this regime, apparently in a rather independent way, without interfering, possibly because they act on different length scales. To each mechanism a particular correlation function is naturally associated, giving rise to two distinct lengths growing with different exponents. Due to that, dynamical scaling is violated even if $V(r,t)$ and $C(r,t)$ possibly scale separately with respect to $L_V(t)$ and $L_C(t)$.

D. Breakdown of the domains

As discussed above, although thermal fluctuations become relevant in depinning the system, their effect in the previous regimes is basically to produce the coarsening of the planes without dissolving them. This is because, since in the early stage the spins are quite misaligned, both $\bar{d}$ and $\bar{p}$ are rather large and hence according to Eq. (6), the typical rotation angle $\bar{\theta}$ is rather small.

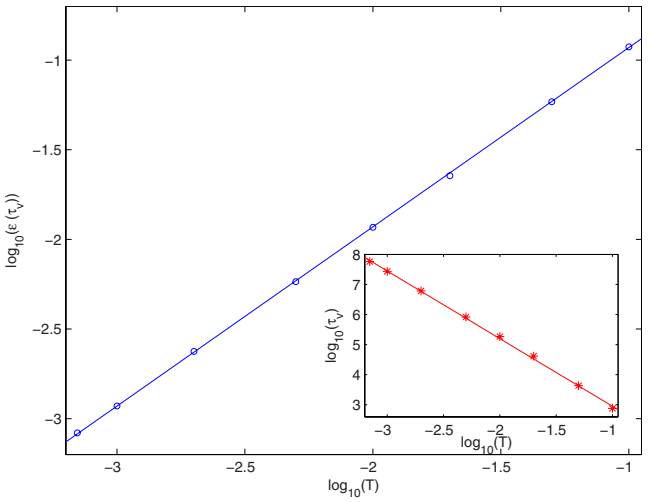

FIG. 8. (Color online) The quantity $\bar{\epsilon}(\tau_v)$ is plotted against T. The continuous line is the best fit $\bar{\epsilon}(\tau_v)=AT$ with $A=2.76$. In the inset $\tau_v(T)$ is plotted against T. The continuous line is the best power-law fit $\tau_v(T)=KT^{-2.3}$.

As the dynamics proceeds, however, textures stretch, spins align, and $\bar{d}$ and $\bar{p}$ decrease. In view of Eq. (6), at a certain time $\tau_v(T)$, values of $\bar{\theta}$ sufficiently large, namely, $\cos\bar{\theta}-1$ of order unity, become available, which are sufficient to destroy the structure of the domains. The breakdown of the planes can be nicely detected by directly looking at the spin configuration or, more properly, by inspection of $V(r,t)$. In fact, while for $t<\tau_v(T)$, $V(r,t)$ takes the scaling form (14), for $t>\tau_v(T)$, when the domain disappears, it quickly collapses to a rapidly decaying function. Meanwhile, $L_V(t)$ stops growing and abruptly decreases, as shown in Fig. 4.

$\tau_v(T)$ can be evaluated by means of Eq. (17). The condition $\cos\bar{\theta}-1 \sim 1$ for the breakdown of the plains is realized when

$$\bar{\epsilon}(\tau_v) \simeq AT, \tag{19}$$

where A is a constant. This is very well confirmed numerically. In Fig. 8, we plot the average energy computed at the time when $L_V(t)$ reaches its maximum against the temperature of the quench. We find that Eq. (19) is well verified with $A \simeq 2.76$.

In order to estimate $\tau_v(T)$ we notice that $\bar{\epsilon}(t)$ is entirely associated with the smooth rotation of the spins in the bulk of the domains, because on the interface between domains spins are perfectly aligned. The typical angle between two adjacent spins is $\bar{\phi} \sim L_C^{-1}(t)$. Hence the energy $\bar{\epsilon}(t)=1-\cos\bar{\phi} \sim L_C^{-2}(t)$, a fact that we have verified with good accuracy in the simulations. This leads to

$$\tau_v(T) \simeq KT^{-\chi}, \quad \chi=\frac{5}{2}, \tag{20}$$

where K is a constant. The dependence of $\tau_v(T)$ on temperature is shown in the inset of Fig. 8. We find a power-law behavior but with a value $\chi \simeq 2.3$ only in rough agreement with the expected value $\chi=5/2$. This partial agreement is

probably due to the fact that our results are only valid in the asymptotic limit of small T and large times t. Here, for instance, we cannot consider very small temperatures since for $T<10^{-3}$ the time of domain breakdown is too long for our simulations. However, as already observed, in such large-temperature regime the numerical data do not scale according to the asymptotic behavior (recall the discussion regarding Figs. 3 and 4 in Sec. III C).

Since the time to approach and leave the frozen state is negligible in the $T\to 0$ limit, $\tau_v(T)$ represents also the duration of the regime where scaling is violated. Notice that it increases quite rapidly as quenches are made deeper.

E. Second phase-ordering regime: Absence of domains

We have seen that the breakdown of the domains occurs when the energy $\bar{\epsilon}(t)$ of the system is comparable to AT ($A \simeq 2.76$) [Eq. (19)]. On the other hand, the system equilibrates at the time $\tau_{\rm eq}(T)$ when $\bar{\epsilon}(t)$ reaches the equilibrium value $\bar{\epsilon}(\tau_{\rm eq})=E_{\rm eq}(T)\simeq T$. Hence the energy must still be lowered after the breakdown of the planes. Then, phase ordering must continue even after $\tau_v(T)$. Clearly, once the domains are eliminated, smooth rotations of the order parameter remain the only mechanism at work, and one expects the usual coarsening mechanism of vectorial systems for $L_C(t)$, characterized by dynamical scaling with $z=4$. This can be checked in Fig. 3. One can observe that the power law (2) continues to be valid, with no apparent modifications, even after the breakdown of the planes, signaled by the decrease in $L_V(t)$ [Fig. 4].

F. Equilibration

Recalling that $E_{\rm eq}(T)\simeq T$, using again $\bar{\epsilon}(t)\sim L_C(t)^{-2}$ one obtains

$$\tau_{\rm eq}(T) \simeq A^2 \tau_v(T). \tag{21}$$

This results shows that the duration of this regime characterized by dynamical scaling is comparable to that of the previous one. Their duration diverges with the same exponent as $T\to 0$.

In the simulations, after $\tau_{\rm eq}(T)$ the system is observed to enter the equilibrium stationary state. Computing the behavior of some equilibrium quantities as, for instance, $E_{\rm eq}(T)$ or $\xi(T)$, we found the exact equilibrium results of Sec. II with great accuracy. This confirms the correctness and the efficiency of the heat-bath transition rates (4).

IV. SUMMARY AND CONCLUSIONS

In this paper we have studied the kinetics of the one-dimensional Heisenberg model with conserved order parameter. The distinguishing feature of this model is the presence of defects in the form of couples of parallel spins separating coplanar regions. These are quite unusual and somewhat counterintuitive defects since normally one associates the notion of defect to regions where the order parameter varies quite abruptly, while here spins are perfectly aligned on the defect. Their nature, however, is clearly manifested in the representation of $\vec{v}_i$, where they qualify as unstable (but long living in deep quenches), pointlike defects. Their presence makes the kinetics similar in some respect to that of a scalar order parameter, because defects play the role of interfaces in the $\vec{v}_i$ representation. In particular, since the removal of defects can only be achieved by activated moves, in a low-temperature quench the system initially pins; the later thermally activated evolution is characterized by coarsening of the domains with the *scalar*like exponent $z=3$. The vectorial nature of the system makes itself manifest particularly in the smooth rotations of the spins inside the domains, producing alignment over a typical length growing with an exponent $z=4$ characteristic of vectorial systems. This interplay between two different ordering mechanisms continues up to a time $\tau_v(T)$ [Eq. (20)], which represents the lifetime of unstable defects. After, defects are removed by thermal fluctuations and a second phase-ordering regime sets in, characterized only by smooth variations of the spins, where dynamical scaling is obeyed. It is worth mentioning that the duration of the second phase-ordering regime, without defects, is comparable with respect to that of the first one in the low-temperature limit.

These features are unusual and unexpected in nondisordered phase-ordering systems. A natural question, therefore, regards their generality, namely, if one could expect a similar behavior in other systems. The peculiar dynamics found in the Heisenberg chain is obviously related to the conserved character of the kinetics. Therefore we do not expect to find something similar in systems without the conservation law, because in that case parallel spins can be singularly updated and, in doing so, the defect is removed. In order to check this we have performed simulations of the system subjected to the same Hamiltonian but with a dynamics which does not conserve the magnetization. As expected, in this case we did not find the unusual features observed with COP, such as scaling violations. The same is found by considering a dynamics where conservation is imposed only globally (by exchanging two spins without the constraint of neighborhood), as expected since it is known [1,18] that the global conservation law is irrelevant. Restricting to systems where conservation is realized locally, as far as we can see there is no reason preventing the formation of similar defects for $N>3$ or, perhaps, even with $d>1$. The other ingredient which turns out to be fundamental in the model considered insofar is the ability of the system to squeeze all the n spins between two defects into a plane, during the regime preceding the pinning. This reduction in the effective internal dimensionality of the order parameter from N to $N-1$ can be achieved because, since n is finite, these spin can be projected on the most energetically favorable plane in a finite time (the time over which the system pins at $T=0$). On lattices, the feature of n being finite is related to the one-dimensional nature of the system. In fact, in $d>1$ the typical configuration of the system is a bicontinuous percolating structure [1] and, even assuming that a relevant number of couples of parallel spins may be formed in an early stage, their geometry should not enclose a domain with a finite number n of spins. Actually, we have run some simulations of the Heisenberg model in $d=2$ and we have not find the peculiarities of the one-dimensional case. On inhomogeneous systems, n is expected to be finite on finitely ramified structures. Therefore, a simi-

lar behavior could be observed on comb lattices, t fractals, and other finitely ramified networks, where phase ordering for discrete models display one-dimensional features [19,20].

On the basis of these reasoning, we also infer that a behavior similar to that of Heisenberg chain with COP could be expected for a generic $\mathcal{O}(N)$ model (with $N \geq 3$) with COP in $d=1$ or, possibly, on finitely ramified networks. Let us mention that our simulations of the $\mathcal{O}(4)$ model quenched to $T=0$ show pinning in states characterized by defects similar to those of the Heisenberg model. A rather complete analysis of the kinetics for generic N, similar to that presented in this paper, is geometrically rather complicated and beyond the scope of this paper, but may represent an interesting issue for further research.

ACKNOWLEDGMENTS

The authors thank Francesco Di Renzo for useful discussions about numerical implementations of the heat-bath algorithm.

[1] A. J. Bray, Adv. Phys. **43**, 357 (1994).
[2] A. D. Rutenberg and A. J. Bray, Phys. Rev. Lett. **74**, 3836 (1995).
[3] H. Furukawa, Adv. Phys. **34**, 703 (1985).
[4] D. A. Huse, Phys. Rev. B **34**, 7845 (1986); J. G. Amar, F. E. Sullivan, and R. D. Mountain, *ibid.* **37**, 196 (1988); T. M. Rogers, K. R. Elder, and R. C. Desai, *ibid.* **37**, 9638 (1988); A. Chakrabarti, R. Toral, and J. D. Gunton, *ibid.* **39**, 4386 (1989); C. Roland and M. Grant, *ibid.* **39**, 11971 (1989).
[5] A. J. Bray, Phys. Rev. Lett. **62**, 2841 (1989); Phys. Rev. B **41**, 6724 (1990).
[6] M. Mondello and N. Goldenfeld, Phys. Rev. E **47**, 2384 (1993); F. Corberi and C. Castellano, *ibid.* **58**, 4658 (1998).
[7] M. E. Fisher, Am. J. Phys. **32**, 343 (1964).
[8] N. A. Lurie, D. L. Huber, and M. Blume, Phys. Rev. B **9**, 2171 (1974); H. J. Mikeska, *ibid.* **12**, 2794 (1975).
[9] G. Reiter and A. Sjölander, Phys. Rev. Lett. **39**, 1047 (1977).
[10] M. E. Gouvea and A. S. T. Pires, J. Phys. C **20**, 2431 (1987).
[11] For instance, in the case of the XY model with non conserved dynamics, we have checked that with the transition rates (4) the asymptotic analytical expressions of Ref. [2] can be verified numerically with great accuracy, while using other transition rates, since the dynamics is incomparably slower, the asymptotic domain is not accessed in any reasonable simulation time.
[12] D. E. Knuth, *The Art of Computer Programming* (Addison-Wesley, Reading, MA, 1997), Vol. 2.
[13] Let us notice that in this case $T=0$ is also the critical temperature of the model. However the kinetics in this case displays all the phenomenology of phase ordering, and not the radically different one of critical dynamics, since the final state toward which the system evolves is completely ordered. A careful discussion of this point is contained in [14].
[14] F. Corberi, E. Lippiello, and M. Zannetti, J. Stat. Mech. (2004), P12007.
[15] A. J. Bray and S. Puri, Phys. Rev. Lett. **67**, 2670 (1991); H. Toyoki, Phys. Rev. B **45**, 1965 (1992); A. J. Bray, Phys. Rev. E **47**, 228 (1993); A. J. Bray and K. Humayun, *ibid.* **47**, R9 (1993).
[16] G. Porod, in *Small-Angle X-ray Scattering*, edited by O. Glatter and O. Krattky (Academic, New York, 1982).
[17] S. J. Cornell, K. Kaski, and R. B. Stinchcombe, Phys. Rev. B **44**, 12263 (1991).
[18] A. D. Rutenberg, Phys. Rev. E **54**, 972 (1996); P. Sen, J. Phys. A **32**, 1623 (1999).
[19] R. Burioni, D. Cassi, F. Corberi, and A. Vezzani, Phys. Rev. Lett. **96**, 235701 (2006).
[20] R. Burioni, D. Cassi, F. Corberi, and A. Vezzani, Phys. Rev. E **75**, 011113 (2007).